Table of Contents

List of Figures

List of Tables

1 Introduction

In addition to behind-the-meter photovoltaics (PV) and battery energy storage systems (BESS), the integration of electric vehicles (EVs) is expected to increase substantially in India in the coming years as a result of clean energy policy targets from the Government of India. The impact of such rapid growth of distributed energy resources (DERs) on the electric grid needs to be understood and quantified to reinforce informed planning and ensure reliable grid operation. To address this, the National Renewable Energy Laboratory (NREL), in collaboration with BSES Rajdhani Power Ltd. (BRPL), has developed an analysis framework that uses state-of-the-art modeling techniques to anticipate the potential impacts on distribution systems in an evolving energy sector. This work is conducted under a broader program, Greening the Grid, which is an initiative co-led by the Government of India's Ministry of Power and the United States Agency for International Development.

This report presents initial findings of the research collaboration between NREL and BRPL and addresses key research questions about the integration of these emerging technologies onto BRPL's distribution grid. The objective is to build a framework for analyzing the economic and technical benefits and challenges of the integration of EVs and BESS and to help optimize infrastructure development costs for BRPL.

1.1 Background

Reducing BESS costs and increased growth in EV penetration are the primary drivers of this research collaboration. BRPL anticipates installing BESS in their distribution transformers (DTs) and a rapid EV rollout soon. BESS deployments and EV rollouts are encouraged by national- and state-level policies to increase renewable integration and reduce emission intensity.

This framework developed by NREL and BRPL captures the combination of this simultaneous evolution (BESS and EV) in distribution system planning so that potential grid impacts can be anticipated, and cost-effective measures can be taken to address potential issues. In addition to developing the framework, NREL adapted grid-readiness metrics that help characterize the scale of system impacts on various measures of grid health.

The cost-benefit analyses of BESS integration are performed on two feeders in BRPL's service territory, chosen for their potential to host a BESS pilot project or strategic investment. Storage technologies are expensive assets and have the potential to provide multiple services to the grid. NREL identifies value streams of utility-scale, grid-interactive BESS for load-leveling applications on transformers, which are similarly applicable across diverse use cases (such as capacity firming and energy arbitrage) for local grid-support services. Along with BESS, realistic models of various EV technologies (such as e-rickshaws and plug-in EVs) are deployed at various penetration levels for public, private, and commercial vehicles. These models will translate the EV fleet on the streets into grid-connected temporal load curves. For techno-economic assessments of grid impacts, this framework computes suites of grid-readiness metrics under different BESS use cases and EV integration scenarios.

Under this collaborative effort with the United States Agency for International Development and BRPL, NREL achieved the following project objectives:

- Developed and validated an accurate and scalable end-to-end framework for simulating various present and future scenarios of the selected feeders

- Developed models to characterize utility-scale BESS operations and economics across different use cases and developed methods to analyze isolated and stacked benefits of the BESS with different control patterns
- Characterized various EV technologies deployed at different penetration levels for public, private, and commercial vehicles in terms of their aggregate demand profiles
- Identified and computed a suite of grid-readiness metrics for techno-economic assessments of network operation impacts under BESS control use cases and EV penetration scenarios
- Defined upgrade requirements for network infrastructure to mitigate possible violations of grid-readiness metrics and reduced potential customer service interruptions caused by an increase in overall system loading from EVs.

These objectives were designed to realize combined value streams of the BESS, which requires careful consideration of use case prioritization, double counts, and time- and location-based constraints. From these analyses, decision makers might benefit from understanding the economic impacts of operational decisions of service providers. Without a robust understanding of trade-offs, during peak periods, for instance, service providers and operators might prioritize load leveling irrespective of how lucrative the energy market prices are within this period. For EV integration scenarios, understanding where, when, and how much consumers charge their vehicles will assist the utility in developing realistic charging-station demand profiles and projections to provide a robust solution for mapping distributed and centralized charging concepts within their service territory. Based on these EV and baseload projections, utilities could develop their network upgrade plans. To that end, NREL carried out sensitivity analyses on possible network upgrades across BESS use cases with stacked benefits valuations specific to the selected distribution feeders.

1.2 Analysis Approach

NREL developed robust simulation-based methodologies and analytic methods for a techno-economic evaluation of grid-interactive energy storage assets across diverse use cases while combining the integration of EV technologies in two selected feeders of the BRPL network. This approach also required maintaining grid reliability and resilience.

This framework can help utilities analyze their network readiness for emerging technologies, the impact of EV penetration on the grid, and the potential solutions introduced by front-of-the meter BESS. Together with technical benefits, this framework allows for an assessment of the economics of conventional (lines/transformers) and advanced network upgrades (storage). Case studies for this framework are designed around New Delhi feeders under various levels of projected growth in EV penetration and charging scenarios.

1.3 Use Cases

This research evaluates the interactions between BESS and EV technologies across diverse use cases and penetration levels, as shown in Figure 1.

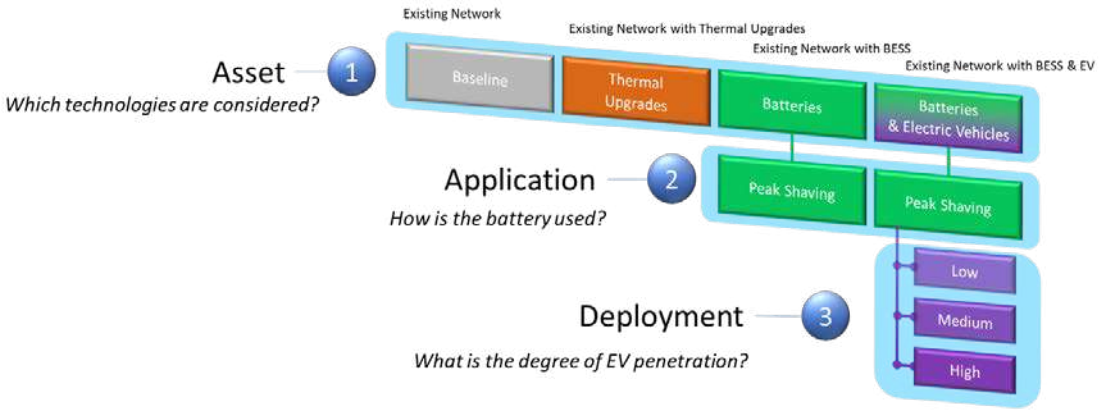

Figure 1. Different use cases and scenarios to consider for the EV/BESS pilot

To obtain all combinations of these technologies, NREL performed the study under a bassline and three major use cases:

1. Baseline: The baseline scenario uses the existing network architecture and feeder loading, which helps differentiate the changes caused by new technologies on the local grid in the subsequent simulation scenarios.
2. Traditional upgrades: This use case considers line or transformer upgrades as needed to prevent network violations. Yearly load growth can exacerbate network operation and cause thermal violations for these devices.
3. BESS and control applications: This use case considers utility-scale BESS, sized as recommended by BRPL, on the baseline model. The intent is to analyze and evaluate the achievable value streams from the integrated energy storage asset. Peak shaving is considered with staged (yearly addition of battery packs) and fixed deployment strategies. EVs are not included in this use case.
4. EVs: Varying levels of EV penetration are considered in this use case. Two subcategories of this use case are:
    A. With peak-shaving BESS
    B. Without BESS (baseline and with traditional upgrades).

    Each subcategory considers three EV penetration levels: low, moderate, and high. Initial assumptions for these levels come from the total number of vehicles within the territories of the given feeder(s). Because these scenarios represent future scenarios, corresponding load growth and expected PV are also considered.

These use cases are included as layers on base feeder models, as shown in Figure 2. Any existing DERs can be integrated in the net load layer.

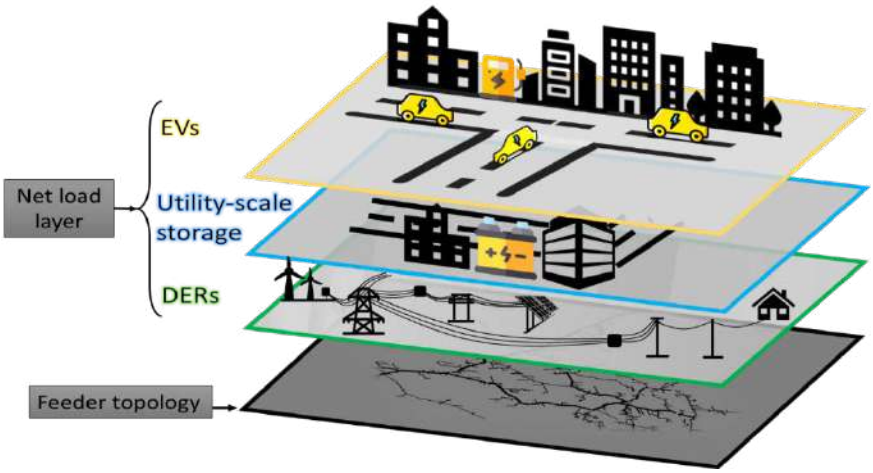

Figure 2. Various layers for modeling loads, EVs, and other DERs for centralized charging concept

2 Distribution Feeder Modeling

This chapter describes the methodologies used for building analyses-ready feeder models, including allocating and cleaning data for the EV integration and BESS impact studies. Two distribution feeders (Feeder 1 and Feeder 2) in Delhi were identified by BRPL and were therefore selected as case studies to better understand the impact of BESS and EVs. Using the topological and network configuration data provided by BRPL, NREL modeled the network in OpenDSS, an open-source software for simulating electric distribution systems.

2.1 Distribution System Analyses Tool

For the purpose of performing distribution system power flows OpenDSS is used. The OpenDSS is a comprehensive electrical power system simulation tool for electric utility power distribution systems. It supports nearly all frequency domain (sinusoidal steady-state) analyses commonly performed on electric utility power distribution systems. In addition, it supports many new types of analyses that are designed to meet future needs related to smart grid, grid modernization, and renewable energy research. Primary purpose to choose OpenDSS is that OpenDSS is designed to be scalable so that it can be easily modified to meet required needs as opposed to other off-the-shelf solutions such as Synergi, CYMEDIST.

2.2 Distribution Network Modeling

The building blocks of this feeder analysis framework require multiple data sets to be compiled into a usable distribution network model, as shown in Figure 3. The network topology is created from the geographic information system (GIS) database that manages all network assets. Equipment databases are used to identify and model attributes of different network assets, such as distribution lines, transformers, capacitor banks, and existing PV systems. Demand is also a critical component of this model. Base demand profiles are created from supervisory control and data acquisition (SCADA) data and consumer energy consumption patterns.

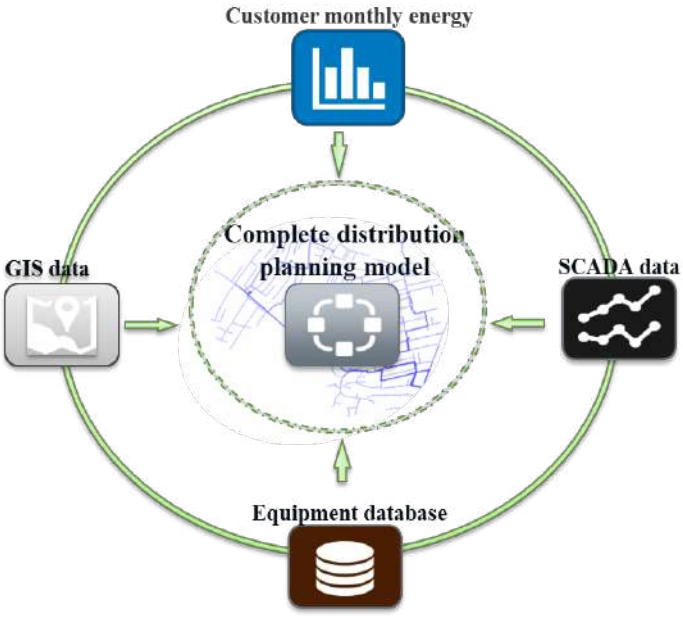

Figure 3. Network model development for the planning framework

In many instances, utilities do not have real electric models for network segment modeling, simulation, and power flow studies. Instead, they maintain a GIS database to manage network assets for their service territories. A pivotal step to enable accurate characterization of feeder operations is to convert the GIS data into a format suitable for OpenDSS. GIS-based shapefiles provide visualization for the feeder topology and typical path and engineering design of wires and towers (Stephen, 2014); however, a critical issue with GIS-based network diagrams is in the accuracy of network segment connectivity. For example, line segments that appear to be connected in GIS visualization could be separated by a minute distance, which might not be obvious to visual perception and therefore might result in an unsuitable model for power flow analysis (Espinosa, 2015).

2.2.1 Converting Geographic Information System Files to a Connected Network

The distribution network segments are represented within the GIS database by layers, which have different numbers of features (i.e., attributes) and geometry types, as shown in Table 1. These data layers are processed in QGIS software, an open-source platform to analyze and visualize geospatial information.

Table 1. Features and Types of Network Segments

Layer ID	Layer Name	Number of Features	Geometry Type
0	Busbar	69	Line string
1	Circuit breaker	23	Point
2	Distribution transformer	7	Point
3	Extra-high voltage lines	1	Polygon
4	High-tension cable	21	Line string
5	Low-tension cable	27	Line string

6	Overhead conductors	165	Line string
7	Substation	7	Polygon
8	Switch	60	Point

The QGIS software uses line strings to represent line segments in the network, some of which are polylines, as shown in Figure 4 making it difficult to access all the features of each segment. Also, these polylines, which are continuous lines with one (or more than one) line segments, are represented as a single object in QGIS. These polylines have a single source and end point coordinates, which do not fully represent them and are therefore insufficient to build electrical models in power network modeling and simulation tools.

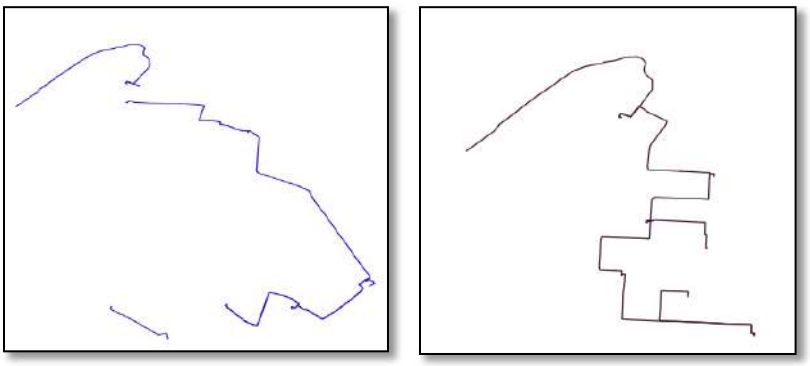

Figure 4. Line string example of feeder sections with multiple polylines

To address the issue with polylines, the following procedure was implemented in QGIS:

1. Explode each line layer. This takes each line and creates a set of new lines representing segments of the original line. The new lines have a start and an end point without intermediate nodes.
2. Export the geometry of the exploded layer to nodes and attribute files using the MMQGIS plugin. The resulting line segments from Step 1 have nodes with source and end coordinates.
3. Add the coordinates of all the line layers from Step 2 to form the network line topology as shown in Figure 5 and Figure 6 for Feeder 1 and Feeder 2, respectively.

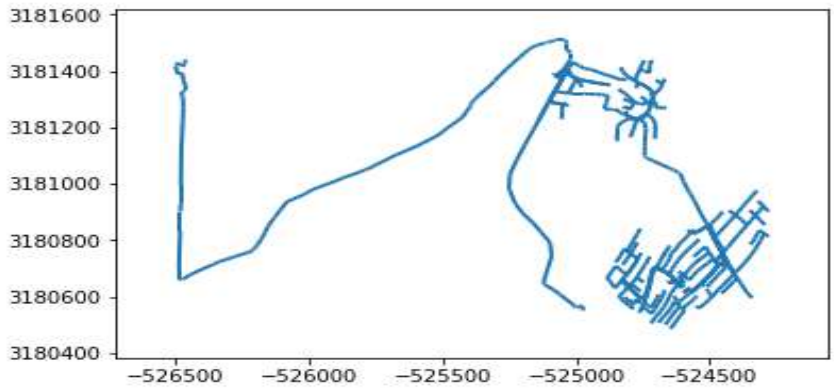

Figure 5. GIS-based reconnection model for Feeder 1

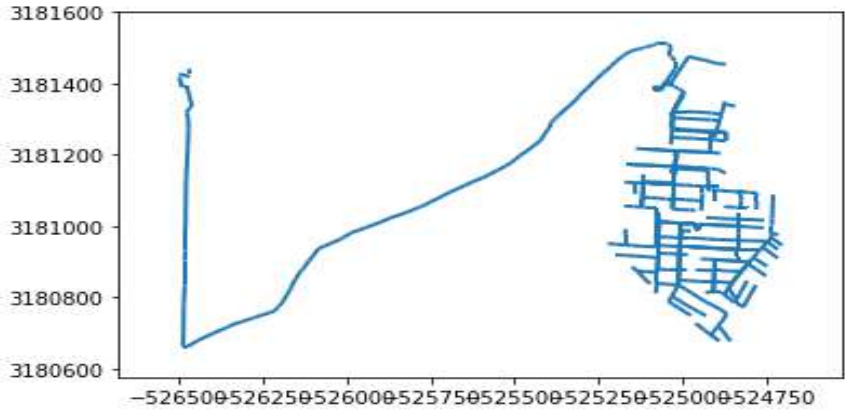

Figure 6. GIS-based reconnection model for Feeder 2

2.2.1.1 Network Creation

This section describes the feeder reconnection process from the GIS-based shapefiles using node coordinates obtained from the distribution utility coupled with the corresponding attribute table to perform the following operations using the NetworkX package.

2.2.1.1.1 Edge Creation

To create edges for nodes with various line layers of the feeder—such as underground, overhead, low-tension, and high-tension—the edge parameters are defined to capture the different line characteristics. Some considered parameters include capacitance, continuous line ratings, positive-, negative-, and zero-sequence impedances. Cables used for edge creation are classified according to their size and voltage level (e.g., 11 kV, 415 V). Also included in this class are distribution transformers for connecting nodes, whose parameters are defined such as the connection types, windings, maximum and minimum taps, and percentage load and no-load losses.

2.2.1.1.2 Feeder Head Location

The feeder head is determined by identifying any node within the vicinity of the substation with only one neighbor connected. This procedure was implemented by constructing a rectangle with the substation nodes and then identifying the node with one neighbor connected to it.

2.2.1.1.3 Adding Nodes and Merging Neighboring Nodes

The next step is combining the nodal elements—such as the circuit breakers, distribution transformers, and switches—with their properties in the attribute table for the respective feeders. For circuit-breaker nodes, attention was given to never use bus bars as an edge parameter because they are internally connected, as shown in Figure 7. Figure 8 shows distribution transformers connecting overhead lines for a certain portion of the feeder.

To determine if nodes should be merged, the Euclidean distance metric (D) was used to compute the distance between nodes. Nodes with $D < 0.001$ are considered neighboring nodes and are thus merged into a single node.

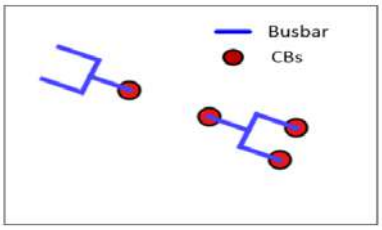

Figure 7. Bus bar and circuit-breaker connection

2.2.1.1.4 Remove Loops in Feeder Layout

There is a high possibility of forming loops or cycles in the process of network creation. For instance, circuit-breaker nodes can easily form a loop that causes power flow to be trapped in a section of the network with a high tendency to increase network losses. To remove these cycles, edges connecting circuit breakers to create loops are removed from the network topology.

Because power flow cannot run in a disconnected network, it is important to compute the number of connected and disconnected components. To determine the main connected components, a list of connected components generated as subgraphs was created. Not all disconnected line segments or nodes can be fixed automatically or algorithmically. Reconnecting components that are disconnected might require human intervention to decide whether to connect islanded components. In some cases, axis coordinates are flipped to connect disconnected line segments.

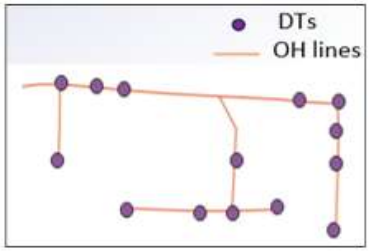

Figure 8. Distribution transformers connecting overhead lines for a certain portion of the feeder

The complete procedure for translating GIS data to the OpenDSS format is illustrated in Figure 9. The reconnection models are updated with a device data sheet to create the OpenDSS model, with the load profiles as inputs to the OpenDSS model.

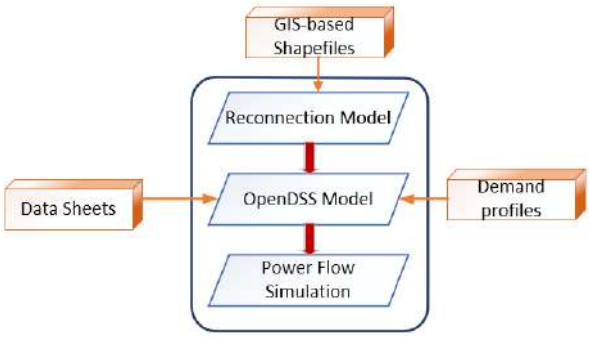

Figure 9. GIS-based data set translation to OpenDSS model

2.3 Distribution System Loading Data Sets

We received three loading data sets from BRPL: (1) three-phase, three-wire, 2-W metered data obtained at both 11-kV feeder heads; (2) three-phase, three-wire, 3-W metered data obtained at all distribution transformers; (3) and monthly customer billing data.

2.3.1 Feeder Head Loading Data

BRPL shared feeder head loading data sets for Feeder 1 and Feeder 2 that included time series of import and export readings, Phase A and Phase C voltage readings (kV), current readings (A), demand (kW), the power factor, and the time stamp. All these data were sampled at a time resolution of 15 minutes and span 1 year: from October 30, 2017, to September 30, 2018.

Figure 10 shows the combined loading of Feeder 1 and Feeder 2. Peak loading is observed in the evening hours during the summer months, and the lowest loading conditions are during the early hours during the winter months.

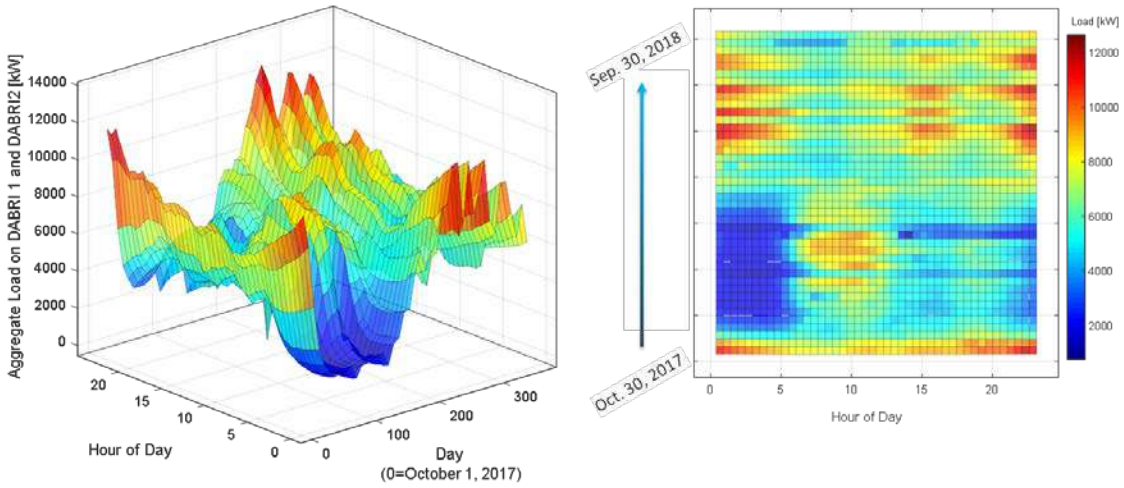

Figure 10. Surface plot of aggregate demand on Feeder 1 and Feeder 2 showing diurnal and seasonal variability (left) and heat map of aggregate demand on Feeder 1 and Feeder 2 showing diurnal and seasonal variability (right)

2.3.2 Distribution Transformer Loading Data

NREL received seven distribution transformer loading data sets for both Feeder 1 and Feeder 2, for a total of 14 distribution transformer loading profiles. Each data set comprises time-series data that include the

active power, reactive power, and voltage on each of the three phases of the secondary distribution lines spanning the same year as the feeder head time-series data. A time series that indicates outages is also included.

2.3.3 Customer Billing Data

In addition to the feeder head and distribution transformer loading time-series data sets, BRPL provided the customer billing information for all customers serviced by each distribution transformer.

2.3.4 Method for Cleaning Distribution Transformer Data

The distribution transformer data are cleaned to enable the quasi-static time series simulations. Once cleaned, the time series are normalized relative to the maximum loading condition observed on each distribution transformer. The data cleaning process is described in the following sections.

2.3.4.1 Data Cleaning Process

The data were analyzed to decompose the typical trends in the loading profiles from the abnormal variabilities including measurement errors. Typical trends are a composite of several timescales; load variability features subhourly, hourly, diurnal, and seasonal dynamics. Here, we focus on the daily trend, which is characteristic for each month of the year; and the seasonal variability, which is characterized by a daily relative drift from the mean monthly value.

To obtain the typical daily profile for each month, the loading observed during each half-hourly time point is averaged with all the same half-hourly values within the month (e.g., all points at 1:30 a.m. in April are averaged for a single value for April, 1:30 a.m.). This process is repeated for each month in the year, producing a profile that is used as a template, or donor, profile to fill missing time points. The donor profiles for Feeder 1 and Feeder 2 are shown in Figure 11 and Figure 12.

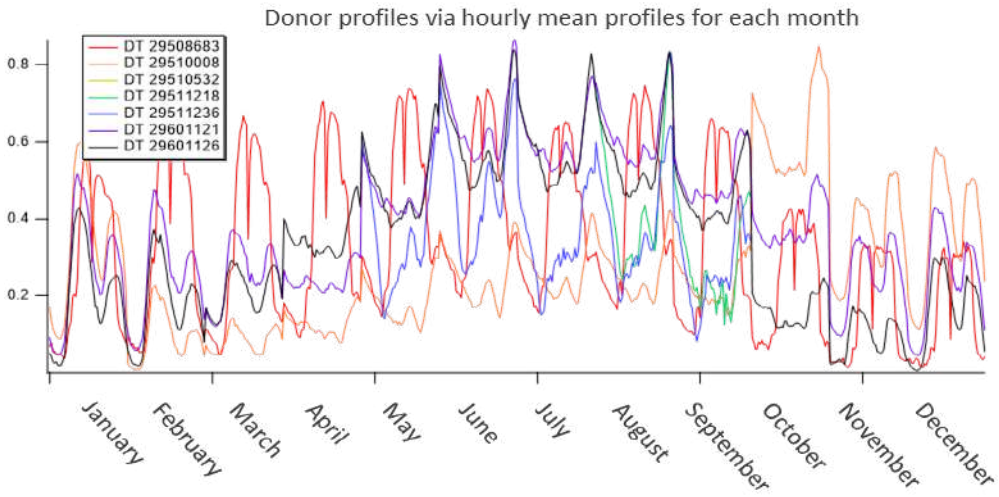

Figure 11. Donor profiles for each distribution transformer for Feeder 1 during each month

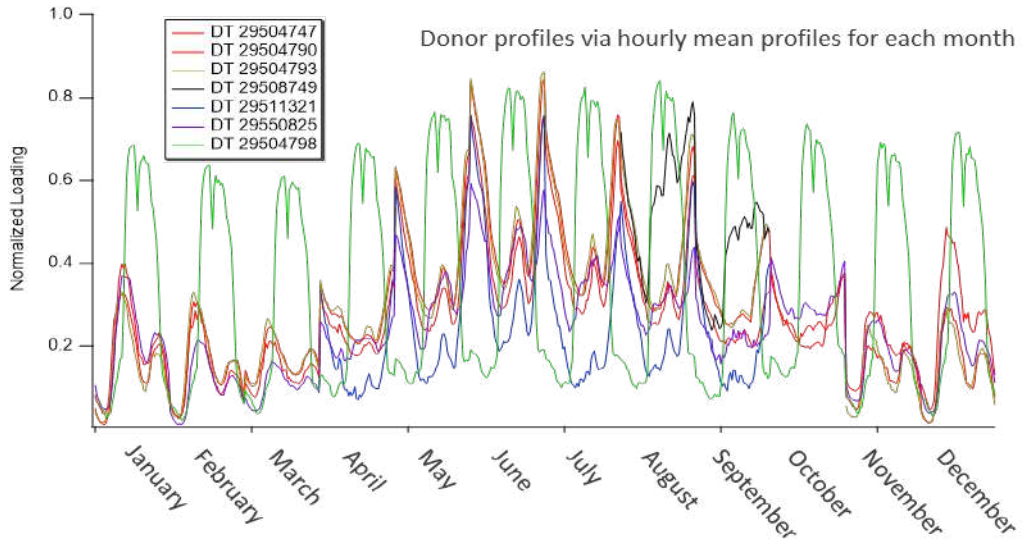

Figure 12. Donor profiles for each distribution transformer for Feeder 2 during each month

Some notable consequences of using a donor profile to fill in the missing data include that the data at the boundaries of the domain of the missing data might feature a step discontinuity. A smoothing technique is used to prevent this. Additionally, if a single donor profile is used repeatedly to fill consecutive days, those days would not feature seasonal variability and inter-monthly trends. To incorporate more natural variability into the data sets when there are large gaps, the daily mean drift from the monthly mean value interpolated to a 30-minute resolution and expressed as a percentage is used as an alternative to duplicate days being repeated. The filled data taken from the donor profile are then scaled by this drift factor.

The effect of the daily mean drift and smoothing is shown in Figure 13. This figure shows an instance where there were several consecutive data with afflicted data points that were replaced by synthetic data. Although each day has a similar profile, the scale and absolute load differ slightly throughout the synthetic profile.

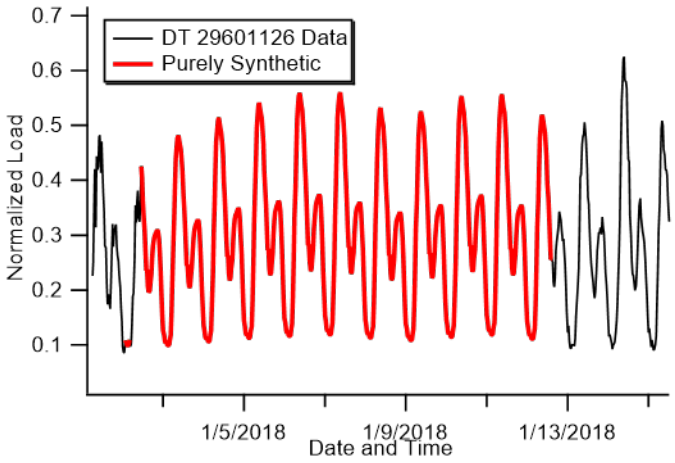

Figure 13. Purely synthetic data filled using the fill processes for DT 29601126 in Feeder 1

The result for each distribution transformer represents a single, serially complete time series that is normalized relative to the maximum loading condition for each transformer. All the various afflictions were removed and replaced with the donor data rescaled by the daily mean drift relative to the monthly mean. In cases where no donor profile data were available, the mean of the remaining distribution transformer profiles was used. Again, a smoothing method was used to avoid step discontinuities.

2.3.4.2 Initial Validation

To validate the data cleaning method, some of the available data were removed so that synthetic data could be compared against the real data. The residuals between the synthetic data and the real data were calculated to ascertain the accuracy of the synthetic data. The distribution of these residuals normally has a mean bias error of -0.036, or -3.6%, as shown in Figure 14. Figure 15 shows the distribution transformer loading profile for DT 29601126 after this data filling method has been applied, and the performance of this method is shown in the green traces (filled in synthetic data) compared with the black ones (real data).

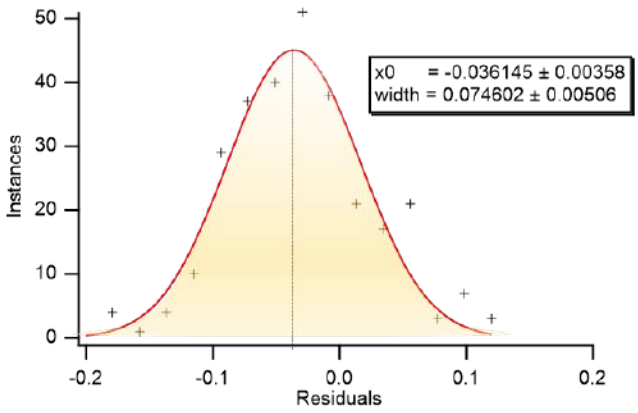

Figure 14. Distribution of residuals obtained by comparing the synthetic data to the real data

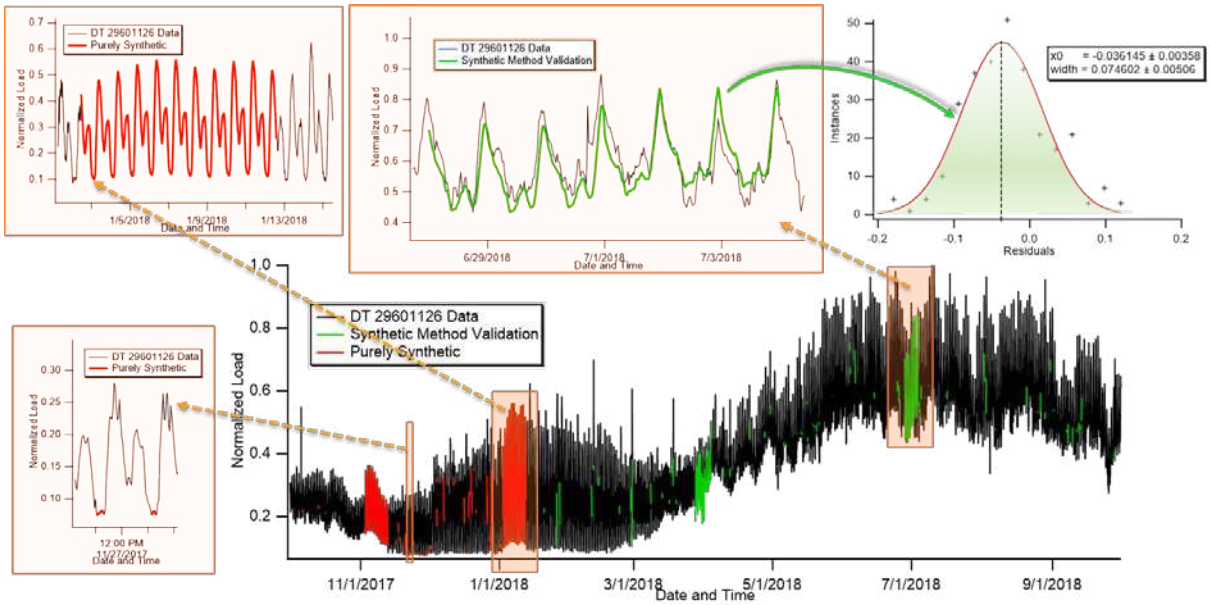

Figure 15. Loading profile for DT 29601126. The green trace represents data that are synthetic and for which real data are available; the red trace represents data that are purely synthetic, i.e., no real data are available.

2.4 Load Allocation

Once the feeder topology has been defined, the next step is to accurately define the secondary loads. This is required because the feeder load along with the circuit impedance will define the power flows. Determining these customer peak load values is both critical and challenging because advanced metering infrastructure and SCADA data are, at this time, usually only available for the substation or, at best, for the distribution transformers, but not for individual customers. To add to this challenge, secondary customers might be moved to different distribution transformers because of changes in demand or network upgrades during the study period. These changes might not necessarily get updated in the utility's GIS, and secondary customer locations might not have been mapped at all. This section describes a method to capture the phase customer load once the per-phase impedance of each circuit component is accurately modeled using the methodology described in the previous section.

Three data sources were available for the load profiles: (1) SCADA data for the feeder head (66/11-kV transformer), (2) the distribution transformers (11/0.433-kV transformers), and (3) monthly kWh values from the billing data for each of the 12 months considered in the study for all customers downstream of the distribution transformers. No information was available for the geographic coordinates of each customer or to which phase they were connected. The following section describes the process for identifying locations and peak load values for all secondary connected customers and validating the resulting customer loading profiles.

2.4.1 Load Allocation Using Individual Distribution Transformer Data

We use the peak-loading condition obtained from each distribution transformer's 30-minute resolution loading profiles to help allocate loads to the secondaries. This is done by using a known parameter—phase voltages—to iterate through a power flow model until loading estimates produce the target voltage. Few distribution transformers experience peak demand at the same time points; therefore, multiple time points corresponding to each distribution transformer's peak-loading condition were analyzed and iterated. The following sections describe the algorithm used and the initial assumptions.

Because of data issues, the voltage drops from the feeder head to the distribution transformer secondaries obtained from power flows on the feeder model did not match with the actual voltage measurements. This is because the same primary cable was supplying the load for all distribution transformers from the feeder head, so if the overall loading differed because of missing data, the voltage drops would also be different. Thus, it was essential to develop an approach to allocate loads to distribution transformer secondaries that could generate the same voltage drops as observed in the measurements while ensuring that the distribution transformer peak loading and phase imbalances are accurately captured.

2.4.1.1.1.1 Using Evolutionary Algorithm for Load Allocation

The voltage drops along a line are based on the real and reactive power flows. The values of these flows are dependent on the system impedance, which had already been captured using the GIS data and component specification sheets, and the values of the secondary loads and power factors on each phase. The approach adopted was to optimally allocate the secondary loads to each distribution transformer at its peak-loading time point using an evolutionary algorithm. An evolutionary algorithm is a generic population-based metaheuristic optimization algorithm.

In this approach, each distribution transformer was allocated optimal loads separately. The per-phase load and power factor values of DT_{opt} (DT being allocated optimal loads), were chosen using the evolutionary algorithm at its peak-loading condition, t_p. Throughout the optimization process, the per-phase load and power factor values of all other distribution transformers in the feeder were kept fixed at the same values as given in their loading profiles at t_p. If any of these inputs were not available, the following assumptions were used to fill in the missing values:

- If the measured loading kW value was zero for any one phase of a distribution transformer, the sum of the other two phases was equally divided in all three phases.
- If a load's kW value was zero or negative (bad data), or if the values were not available for all three phases, then the distribution transformer was assumed to be 50% loaded.
- If the loading values were not available for all three phases of DT_{opt}, then the evolutionary algorithm could choose loading values from ±25% of its rating, else bounds were kept as ±25% of its actual peak-loading value.
- If voltage measurements were not available for one phase, then a reasonable value based on the other two phases was applied.

- If none of the voltages were available, or if they were negative or much lower than nominal, then a value of 1 p.u. or slightly less than the feeder head value was assumed.
- Similarly, if power factor values were not available for one phase, a reasonable value based on the other two phases was applied; if none of the values were available, unity power factor was assumed.

Once these missing values were filled in, the following evolutionary algorithm steps were implemented to get the optimal loads:

- The feeder head voltage in the OpenDSS models are set to the same values as observed in the feeder head SCADA data for *tp*.
- The initial population was then generated for DT_{opt}; here, initial population means a set of values for the loads and power factors for each phase of DT_{opt}. These values were generated from within the specified bounds. The load kW values could be chosen from within ±25% of the measured kW values at *tp*. The power factor values could be chosen from (0.8,1), typical residential power factor values. The distribution transformer tap positions were not continuous and could be chosen from only seven allowed positions (0.9, 0.925, 0.95, 0.975, 1.0, 1.025, 1.05), as given in the distribution transformer specification sheets.
- The initial population consisted of multiple sets of values, and each set was used to evaluate the fitness function. The fitness or the objective function was the squared sum of differences between the target (VT) and actual (VA) voltages for each phase of DT_{opt}. The target voltage was read from the measurements at *tp*, as shown in Figure 16. The actual voltages were obtained by attaching lumped loads at the secondaries of DT_{opt}, with kW and power factor values taken from the initial population sets.

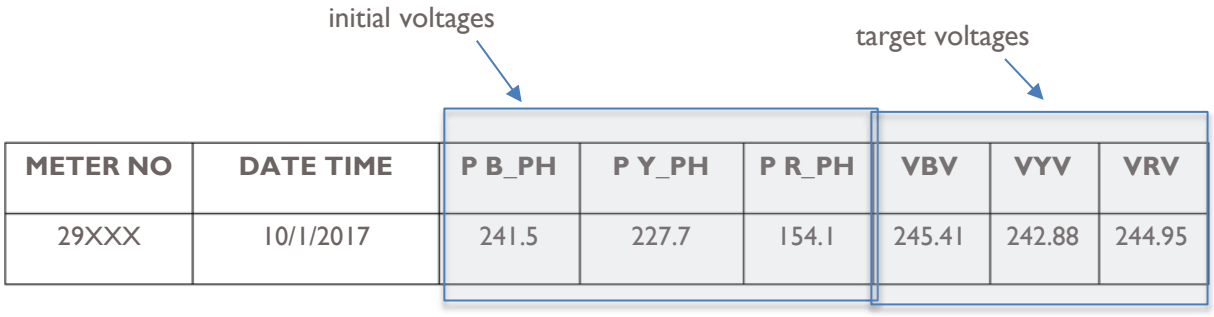

METER NO	DATE TIME	P B_PH	P Y_PH	P R_PH	VBV	VYV	VRV
29XXX	10/1/2017	241.5	227.7	154.1	245.41	242.88	244.95

Figure 16. Initial and target voltages from distribution transformer measurements

The set that gives the least value of the objective function is used to generate the next generation of load kW and power factor values. The DT_{opt} secondary loads are replaced with these values, and the objective is evaluated again. This process is repeated until the difference between the last and current iteration is less than the specified tolerance. The process flowchart is shown in Figure 17. This process is applied to each distribution transformer to generate the optimal peak-load kilowatt, power factor, and tap position values.

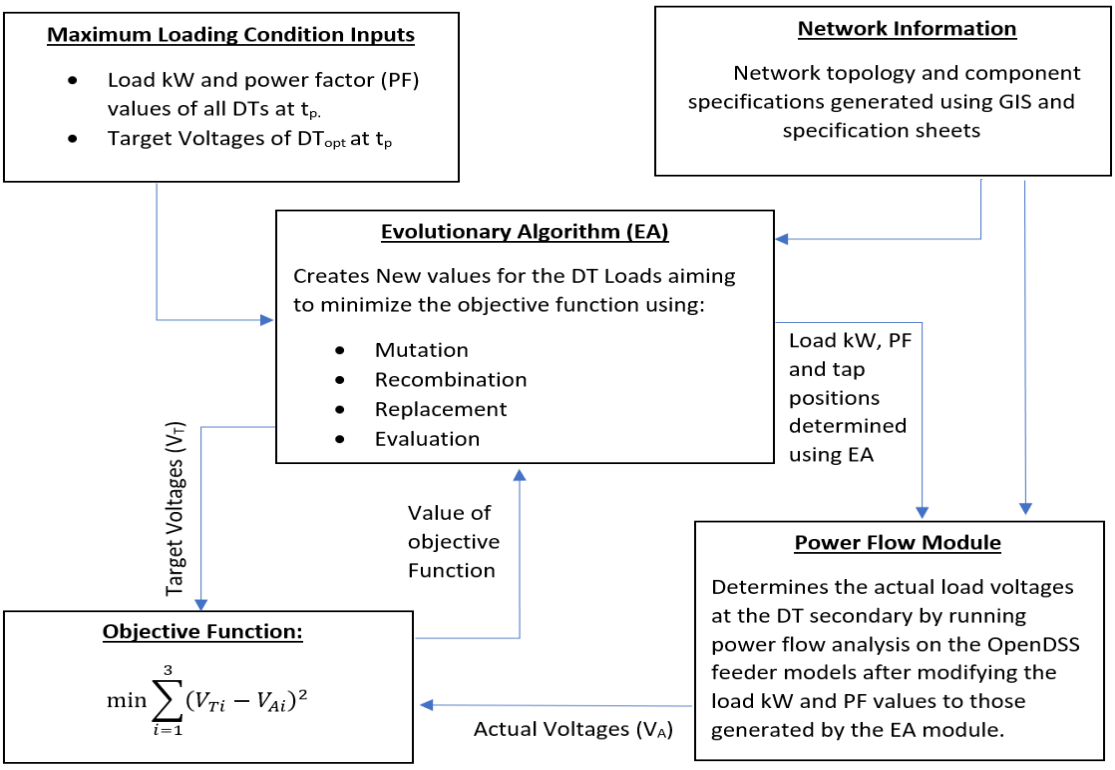

Figure 17. Flowchart of load allocation using evolutionary algorithm

Figure 18 and Figure 19 show a comparison of voltages obtained using this modified approach. The optimal voltages exactly match the target voltages for most distribution transformers and are closer to the target voltages than the initial voltages for others. The reason these values do not exactly match is that other than the assumptions used for filling in missing data, the taps could be chosen from a fixed set of values, and their positions could not be set separately for each phase; however, the power factor values and tap positions are all realistic, and voltage drops are closer to the ones actually observed.

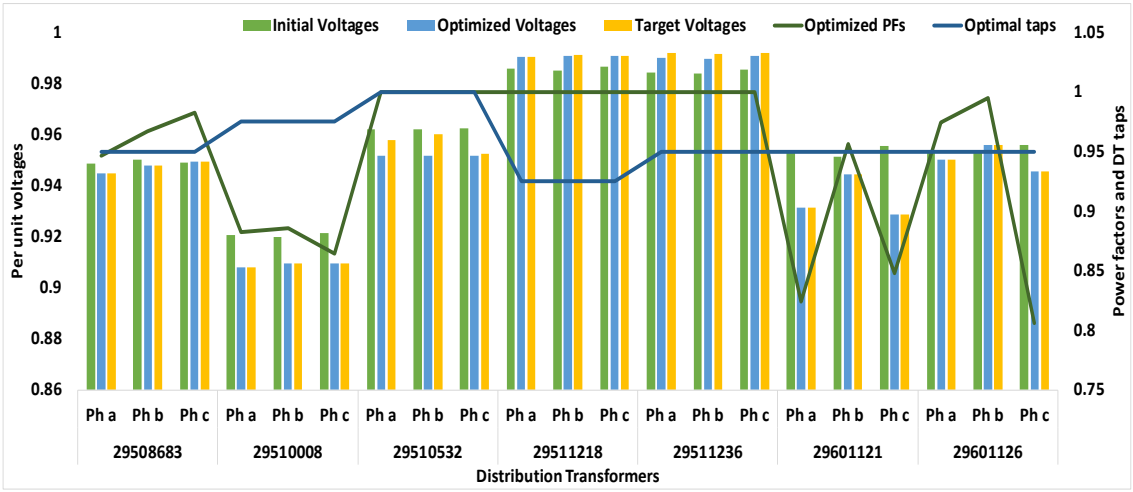

Figure 18. Comparison of voltages using modified evolutionary algorithm for Feeder 1

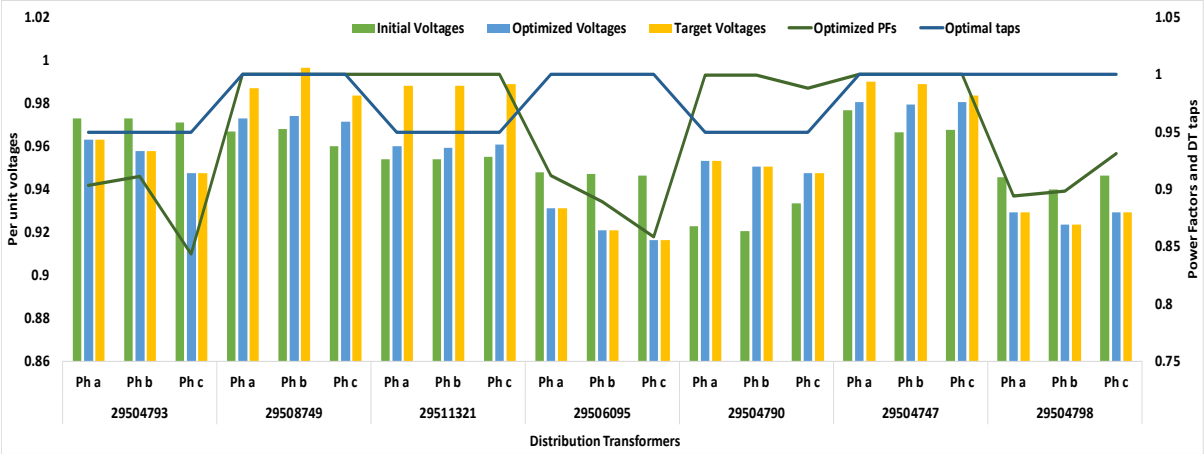

Figure 19. Comparison of voltages using evolutionary algorithm for Feeder 2

2.4.1.1.1.2 Secondary Customer Load Allocation Using the Optimal Lumped Loads

The load allocation optimization algorithm described previously determined the optimal loading values at the secondary of the distribution transformers. These loads give the same voltage drops as given in the measurements and validate the accuracy of the network models to the distribution transformer secondaries; however, these optimal loads represent the sum total of all the loads present downstream of the distribution transformers. Because most EV integration will happen at the individual customer locations, it is essential to distribute these lumped loads on each phase of the distribution transformer secondaries to downstream customers.

Figure 20 shows the feeder models with all the distribution transformers marked as red triangles. These models show that the secondaries represent a significant portion of the feeders; however, further validation of the secondary models was not possible because no information was available for the locations of the secondary customers or their voltage measurements. The only information available was the number of downstream customers for each distribution transformer and their respective monthly kWh values. These values were used to distribute the lumped optimal loads to downstream customers. The approach followed here ensured that the voltage drops and phase imbalances at the distribution transformer secondaries will remain similar to the ones observed from the measurements. This approach is shown in Figure 21.

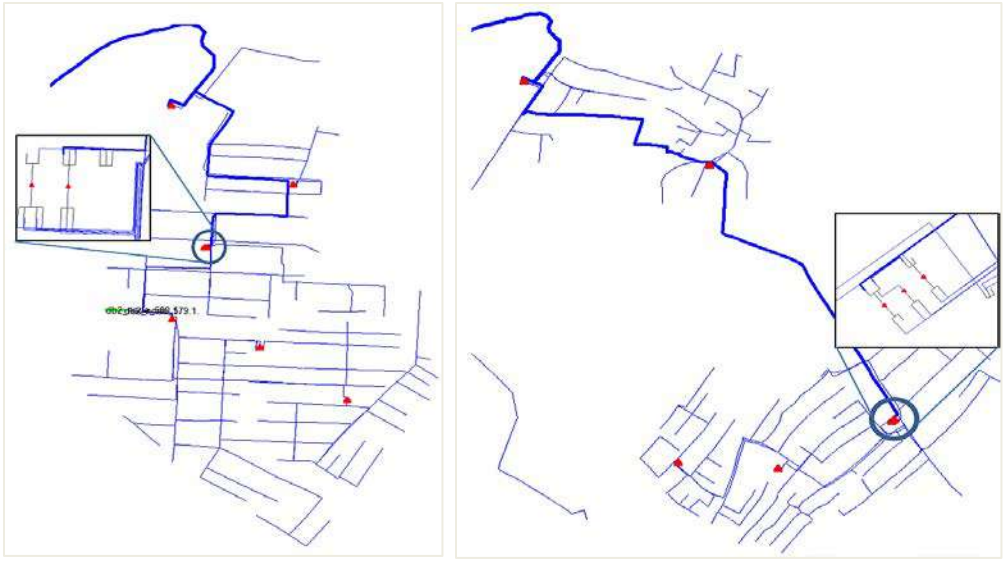

Figure 20. Feeder models showing the primary and secondary networks separated by the distribution transformers (red triangles)

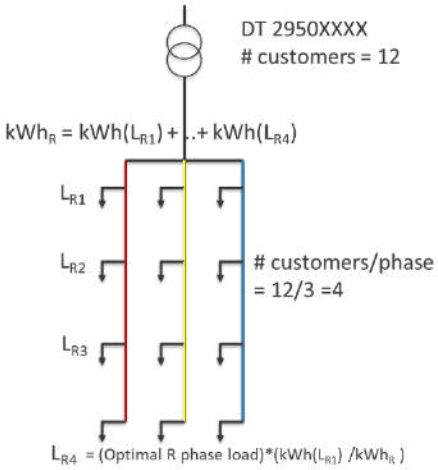

Figure 21. Distribution transformer secondary optimal lumped load among downstream customers

- Because no information was available about which phase the customer was connected to, it was assumed that the number of customers per phase were equal, and the total number of customers for each distribution transformer was divided equally in all the three phases.
- The annual kWh values were then determined for each customer (kWh_{cust}) by summing the monthly kWh values. This averaged any inconsistencies that might have existed in the monthly billing periods and the SCADA data used.
- The lumped load was then distributed to each customer based on their kWh proportion. To implement this, the total annual kWh per phase of the distribution transformers (kWh_{phase}) was determined by summing the annual kWh values of all customers on that phase. Then, for each customer, kWh_{cust} was divided by kWh_{phase} to get the customer's kWh proportion. This proportion was then multiplied by optimal lumped load to get the customer's peak kW value. This ensured that the total load per phase of the distribution transformer stayed exactly the same and the customer's peak loading corresponded with its annual energy consumption.

- The power factor values for each secondary customer load were kept the same as their correponding lumped load's power factor at t_p. Finally, because no nodes existed in the GIS files to connect these secondary customers, addditional nodes needed to be created. These nodes were kept roughly equidistant, and the distance was based on the plot sizes observed in the Google Earth overlay. The newly created secondary nodes are shown in Figure 22.

Figure 22. Feeder 1 GIS layout without secondary nodes (left) and its OpenDSS models with added secondary nodes (right)

3 Grid-Readiness

Evaluation of grid performance is essential for determining the readiness of the grid to adopt emerging technologies. Grid-readiness metrics measure the impact from emerging technologies on the reliability of the network under changing conditions, which is critical when evaluating new investments, large shifts in demand patterns and composition, or untested technologies. As a best practice, the evaluation and development of these metrics relies on time-series data collected from multiyear simulations of feeder models with multiple control schemes. A suite of technical indices is helpful in characterizing and understanding network operations coupled with possible feeder upgrades under different use cases and scenarios. The subsequent sections describe the metrics that are used to evaluate the grid impacts for different use cases and EV integration scenarios.

3.1 Technical Indices

3.1.1 M1: System Average Voltage Magnitude Violation Index

The system average voltage magnitude violation index (SAVMVI) provides a measure of the severity of nodal voltage violations on a bus. It gives an estimate of how far outside the nodal voltages are from their permissible bounds, as shown in Figure 23 (M1), which presents a hypothetical time series and corresponding violations. For this study, separate bounds were used for primary (high-voltage) and secondary (low-voltage) nodes based on the recommendations of the utility. First, all primary and secondary buses were identified. If buses are primary, the overvoltage threshold of V_u = 1.1 p.u. and an undervoltage threshold V_l=0.9 p.u. is used. Similarly, if the bus is secondary then the bounds are assumed to be within V_u = 1.06 p.u. and V_l = 0.94 p.u. A bus could have multiple nodes based on the number of phases, so average bus voltage is considered here:

$$V_i^{avg} = \frac{1}{n}\sum_{k=0}^{n} V_i^k$$

where n is the number of buses in any node *i*.

For each bus *i* at each time point *t*, the violation outside the limits are defined by:

$$V_i^{viol}(t) = \begin{cases} V_{avg}(t) - V_u\,,\ if\ V_{avg}(t) > V_u \\ 0\,,\ if\ V_l < V_{avg}(t) < V_u \\ V_l - V_{avg}\,(t),\ if\ V_{avg}(t) < V_l \end{cases}$$

The time-averaged violation for each bus is then determined by:

$$V_i^{viol\_avg} = \frac{1}{T}\sum_{t=0}^{T} V_i^{viol}(t)$$

where *T* is the total number of simulated time points.

SAVMVI for the feeder is obtained by dividing the sum of the time-averaged violations for all buses by the total number of buses in the feeder,

$$SAVMVI = \frac{1}{N}\sum_{i=1}^{N} V_i^{viol\_avg}$$

where *N* is the number of buses in the modeled network.

For instance, if a feeder has 100 nodes and each node has an average voltage of 1.06 p.u. for all time points (for example, 17,520 time points in total—for 30-minute resolution data set during a year), and the voltage threshold is 1.05 p.u., then:

$$SAVMVI = \frac{(1.06-1.05)*100*17520}{100*17520} = 0.01 \text{ p.u.}$$

3.1.2 M2: System Average Voltage Fluctuation Index

The system average voltage fluctuation index (SAVFI) provides a measure of the differences between average voltages at a current time point and the preceding one (i.e., voltage fluctuations), as shown in Figure 24 (M2). This gives the voltage deviation or fluctuation at all buses at each time point, which is then summed for all the buses across the feeder. The time average for each bus divided by the number of buses gives the SAVFI.

$$V_i^{avg} = \frac{1}{n}\sum_{k=0}^{n} V_i^k$$

where n is the number of buses in any node *i*.

Voltage fluctuation for any bus *i*:

$$V_i^{fluc}(t) = \left|V_i^{avg}(t) - V_i^{avg}(t-1)\right|$$

$$V_i^{fluc\_avg} = \frac{1}{T}\sum_{t=0}^{T} V_i^{fluc}(t)$$

$$SAVFI = \frac{1}{N}\sum_{i=1}^{N} V_i^{fluc\_avg}$$

where *T* is the total number of simulated time points, and *N* is the number of buses in the modeled network.

For example, if the feeder example mentioned in M1 has a constant voltage difference between the previous and current time points of 0.01 p.u., then:

$$SAVFI = \frac{(0.01)*100*17520}{100*17520} = 0.01 \text{ p.u.}$$

3.1.3 M3: System Average Voltage Unbalance Index

The system average voltage unbalance index (SAVUI) provides a measure of the voltage unbalance (maximum difference between a bus's individual phase and average voltage, M3, as shown in Figure 25) among all nodes. Voltage unbalance is defined as:

$$Voltage_{unbalance} = \frac{Maximum\ deviation\ from\ average\ voltage}{Average\ voltage} * 100\%$$

To evaluate the SAVUI for all buses, the maximum deviation of any phase voltage of the bus from the average bus voltage is evaluated at each time point to get the unbalance and is summed for all time points. SAVUI is obtained by dividing the sum of the time-averaged unbalance sums for all buses by the total number of buses:

$$V_i^{avg} = \frac{1}{n}\sum_{k=0}^{n} V_i^k$$

$$V_i^{unb\_max}(t) = \left|\max\left(V_i^k(t)\right) - V_i^{avg}(t)\right|$$
$$V_i^{unb\_min}(t) = \left|\min\left(V_i^k(t)\right) - V_i^{avg}(t)\right|$$

$$V_i^{unb}(t) = \frac{\max\left(V_i^{unb\_max}(t),\ V_i^{unb\_min}(t)\right) * 100}{V_i^{avg}}$$

$$V_i^{unb\_avg} = \frac{1}{T}\sum_{t=0}^{T} V_i^{unb}(t)$$

$$SAVUI = \frac{1}{N}\sum_{i=1}^{N} V_i^{unb\_avg}$$

where n is the number of buses in any node *i*, *T* is the total number of simulated time points, and *N* is the number of buses in the modeled network.

For instance, if a feeder has 100 nodes and each node has an unbalance of 0.01 p.u. for all time points (17,520, as previously explained), then:

$$SAVUI = \frac{(0.01)*100*17520*100}{100*17520} = 1\%$$

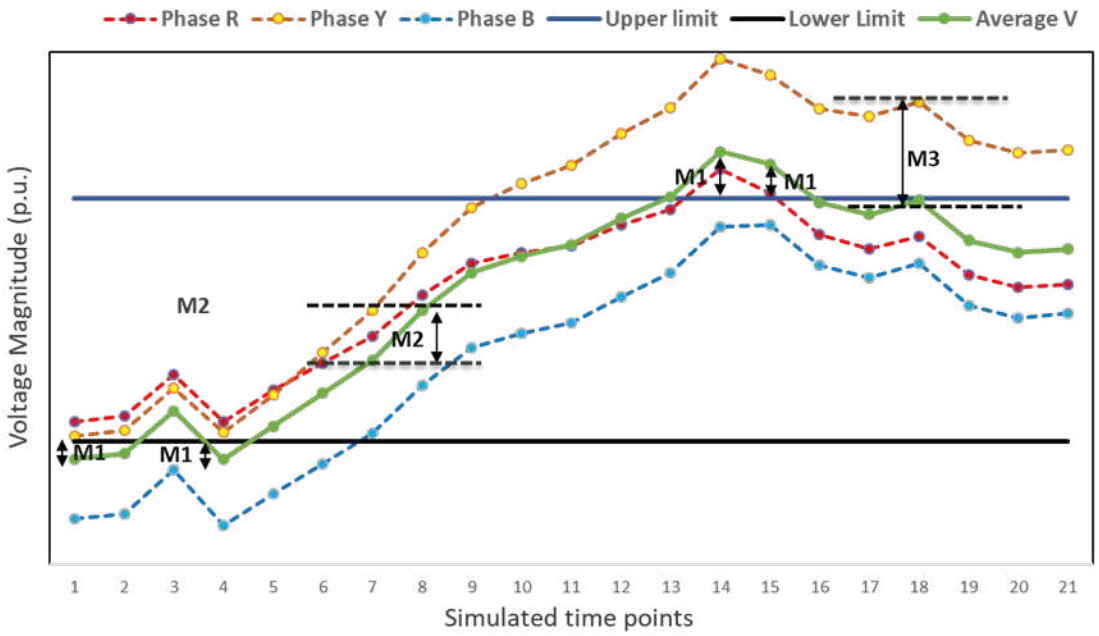

Figure 23. Technical indices used to quantify grid-readiness for hypothetical voltage profiles

3.1.4 M4: System Control Device Operation Index

The system control device operation index (SCDOI) provides a measure of the average control device operations in a day, such as voltage regulators and capacitor banks. For the feeder use cases presented in this report, operations of capacitor banks were evaluated with this index ($SCDOI_{cap}$). $SCDOI_{cap}$ is calculated by summing all capacitor bank operations (TO_{cap}) throughout the simulation time frame and then dividing this net operation count by the number of days (T_{day}) and the number of capacitor banks (*NC*):

$$SCDOI_{cap} = \frac{1}{NC} * \frac{1}{T_{day}} \sum_{i=1}^{NC} TO_{cap,j}$$

For example, if a feeder has two capacitor banks and each capacitor bank operates 10 times in a day, then:

$$SCDOI_{cap} = \frac{2 * 10 * 365}{2 * 365} = 10$$

3.1.5 M5: System Reactive Power Demand Index

The system reactive power demand index (SRPDI) provides a measure of the power factor at the substation and consequently the additional loading on the substation transformer because of reactive power demand/injections of the feeder. To calculate this metric, the absolute reactive power flow at the substation is summed at each time point and divided by the total number of time points simulated:

$$SRPDI = \frac{1}{T} \sum_{t=0}^{T} Q_{sub}(t)$$

where T is the total number of simulated time points.

For example, if the absolute reactive power flowing through the substation is 100 kVar at all time points (17,520, as previously explained), then:

$$SRPDI = \frac{100*17520}{17520} = 100 \text{ kVar}$$

3.1.6 M6: System Energy Loss Index

The system energy loss index (SELI) gives a measure of the total energy loss in the feeder as a proportion of the total energy demand of the loads. For this metric, the total feeder loss (kW and kVar) and total load kW and kVar are stored at each time point. These are then summed and multiplied by a multiplier (*mult*) to get the total energy loss and total energy demand of all loads.

$$mult = \frac{\Delta t}{60}$$

where Δt is the simulation time step in minutes.

Total energy loss equals:

$$E_{loss} = \frac{1}{T}\sum_{t=0}^{T} kW_{loss}^{sub}(t) * mult$$

where T is the total number of simulated time points.

Total load energy demand equals:

$$E_{load} = \frac{1}{T}\sum_{t=0}^{T}\sum_{i=1}^{L} kW_i(t) * mult$$

where L is the number of loads in the feeder.

This index is then defined as:

$$SELI = \frac{E_{loss}}{E_{load}}$$

For example, if a feeder has a constant real power loss of 50 kW at each time point, and the sum of loads is constant at 1 MW at each time point, then during a year or 17,520 time points (30-minutes resolution data set):

$$SELI = \frac{(50)*17520}{1000*17520} = 0.05 \; or \; 5\%$$

3.2 Simulation Architecture

Time-series simulations are conducted leveraging NREL's high-performance computing (HPC) systems, which enable the analysis of a wide variety of scenarios and longer time horizons because of the ability to drastically reduce computational time.

Figure 24 shows the different scenarios of multiyear, quasi-static time-series simulations required to assess grid-readiness and test the efficacy of BESS to mitigate possible overloading conditions. All these scenarios require different time resolutions, control modes, varying EV penetration levels, or network upgrades. Considering all these requirements the simulation platform should have the following features:

- Be scalable to allow for the addition of new control modes, feeder models, EV penetration levels, time resolution, and length of simulations.
- Provide the end user with an easy to use interface.
- Be able to start multiple simulations together leveraging all available computational resources and minimize the total simulation time.
- Be able to store all the raw data and processed results and make it readily available in the future.

The simulation platform characterized in Figure 25 makes use of open-source tools such as OpenDSS and OpenDSSDirect.py, which provides a Python-based library interface to OpenDSS. It leverages the HPC resources available at NREL and is capable of starting thousands of quasi-static time-series simulations together. To further increase resource utilization, another open-source Python package, Dask, was used to run many simulations in parallel on the different cores of the same node. All the results are saved in separate directories to avoid overlaps. The platform also includes a Linux-based command line interface that allows the user to start all the simulations for a feeder with a single command line. Owing to its modular nature, new feeders can be added simply, and new control modes can also be easily integrated and simulated using the existing command line interface. By leveraging these capabilities, simulation times can be reduced from weeks or even months to several hours.